International Energy Agency
Energy Conservation in Buildings and in Community Systems
Annex 20: Air Flow Patterns Within Buildings
Subtask 1: Room air and contaminant flow

RESEARCH ITEM 1.46SF

SIMULATION OF SIMPLE (TWO-DIMENSIONAL) TEST CASES

Date: May 1991
Authors: Heikkinen, J., Piira, K.
Technical Research Centre of Finland (VTT)
Laboratory of Heating and Ventilation
Lämpömiehenkuja 3
SF-02150 Espoo
FINLAND

Report No: AN20.1-SF-91-VTT07
Report Type: Annex report
Distribution: Unlimited
Available: From the authors

CONTENTS

International Energy Agency
Energy Conservation in Buildings and in Community Systems
Annex 20: Air Flow Patterns Within Buildings
Subtask 1: Room air and contaminant flow

RESEARCH ITEM 1.46SF

SIMULATION OF SIMPLE (TWO-DIMENSIONAL) TEST CASES

Date: May 1991
Authors: Heikkinen, J., Piira, K.
Technical Research Centre of Finland
Laboratory of Heating and Ventilation
Lämpömiehenkuja 3
SF-02150 Espoo
FINLAND

Report No: AN20.1-SF-91-VTT07
Report Type: Annex report
Distribution: Unlimited
Available: From the authors

CONTENTS Page

1. INTRODUCTION

Computational results of two two-dimensional benchmark cases specified by Nielsen (1990) are presented. The isothermal case (2D1) is suitable for the testing of CFD codes because reliable measurements exist. The aim of the nonisothermal case (2D2) is to predict a strong buoyant effect. Results with the WISH code (Lemaire 1989c) are presented and compared with measured ones given by Nielsen (1990). Some results with the Fluent 2.99 code (Creare 1987) are also given in order to study the effects of the computational grid and differencing schemes.

2. GEOMETRY AND BOUNDARY CONDITIONS

The test room is shown in Fig. 1. The geometry is specified by H = 3.0 m and L/H = 3.0, h/H = 0.056 and t/H = 0.16.

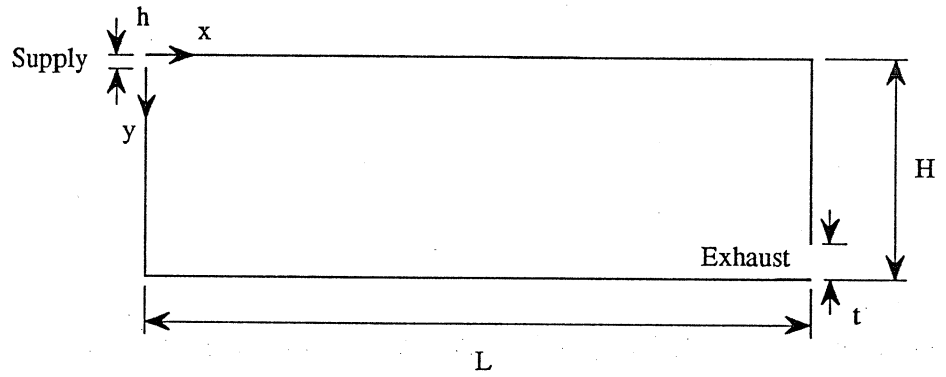

Figure 1. Geometry of the two-dimensional test case

The inlet velocity u_0 is calculated so that the Reynolds number

$$Re = h\, u_0/\nu = 5000$$

will be the same as in model experiments with H = 0.0893 m. In a room with H = 3.0 m supply air velocity has to be u_0 = 0.455 m/s if kinematic viscosity $\nu = 15.3 \cdot 10\text{-}6$ m^2/s at temperature 20 C is used. The inlet conditions for the turbulent kinetic energy k and dissipation ε are

$k_0 = 1{,}5\ (0{,}04\ u_0)^2$ and

$\varepsilon_0 = k_0^{1,5}/l_0$, where $l_0 = h/10$.

For the non-isothermal case Archimedes number Ar is defined as

$$Ar = \beta\, g\, h\, \Delta T_0/u_0^2$$

where β = 1/293K, g = 9.81 m/s^2 and ΔT_0 is the temperature difference between the exhaust and supply.

3. SIMULATION MODEL

A Wish code in the Cray X-MP computer has been used. The code uses the finite volume method described by Patankar (1980). An upwind-differencing scheme is used in representing convective transport. The high Reynolds number k-ε turbulence model (Launder, Spalding, 1974) is used with model constants in Table 1. At the walls beyond the laminar sublayer, a logarithmic wall function is used with von Karman constant 0.4 and smoothness factor E = 9.

Table 1. Diffusion and source terms in the general equation

$$\mathrm{div}\ (\ \rho_o \bar{v}\ \phi - \Gamma_\phi\ \mathrm{grad}\ \phi\ ) = S_\phi$$

ϕ	Γ_ϕ	S_ϕ
v_i	$\mu+\mu_t$	$-\frac{\partial p}{\partial x_i} + (\rho - \rho_o)\, g_i$
h	$\mu/Pr+\mu_t/\sigma_h$	0
k	$\mu+\mu_t/\sigma_k$	$P - \rho_o\epsilon + G$
ϵ	$\mu+\mu_t/\sigma_\epsilon$	$C_1 P\epsilon/k - C_2\rho_o\epsilon^2/k + C_3 G\epsilon/k$

$$P = \mu_t \left(\frac{\partial v_i}{\partial x_j} + \frac{\partial v_j}{\partial x_i} \right) \frac{\partial v_i}{\partial x_j}$$

$$G = - g_i \frac{\mu_t}{\sigma_h} \frac{\partial \rho}{\partial x_i}$$

$$\mu_t = C_\mu \rho_o k^2/\epsilon$$

$$C_1 = 1{,}44,\ C_2 = 1{,}92,\ C_\mu = 0{,}09,\ C_3 = 1{,}44$$

$$\sigma_k = 1{,}0,\ \sigma_\epsilon = 1{,}3,\ \sigma_h = 0{,}9$$

NOMENCLATURE

c_p = specific heat capacity of air (1000 J/kgK)
h = enthalpy = $c_p t$
k = kinetic energy of turbulence
p = air pressure + $2\rho_o k/3$
Pr = Prandtl number of air (0,71)
t = air temperature, °C
x_i, x_j = tensor notation for space coordinates
v_i, v_j = mean velocity in i and j directions
$\bar{v}$ = mean velocity vector
ϕ = general variable
ϵ = turbulence dissipation rate
ρ = air density = $\rho_o(1-(t-20\ ^oC)/293)$
ρ_o = air density at 20 °C (1,2 kg/m^3)
μ = dynamic viscosity of air

4. RESULTS OF THE ISOTHERMAL CASE

The main results can be seen in Figures 2 to 10. They have been computed with the Wish program using a computational grid of 1170 points (= 45x26 in the x and y directions). The grid spacing can be seen in the vector plots. The distance from the first grid point to the surface is 10 mm at the ceiling, 15 mm at the east wall, 15 mm at the floor and 20 mm at the west wall. The velocities have been made dimensionless by dividing by the supply velocity. The velocity fluctuation in the x-direction has been estimated from equation

$$\sqrt{\overline{u'^2}} = \sqrt{k}/1.1$$

which is based on nonisotropy of typical wall jet turbulence (Nielsen 1990).

The decay of the supply air jet is quite well predicted (Fig. 9) up to x/H = 2, where the simulated velocity starts to decrease faster than the measured velocity. Recirculation in the upper right corner is not predicted. Recirculation exists in the lower left corner but it is much weaker than in the measurements (Fig. 10). The location of the maximum velocity near the floor is at the same point x/H = 2.2 in computations as in the measurements but the velocity is 8 % lower (Fig. 10). Turbulence fluctuation is fairly well predicted near the ceiling (Fig. 9) but not so well near the floor (Fig. 10).

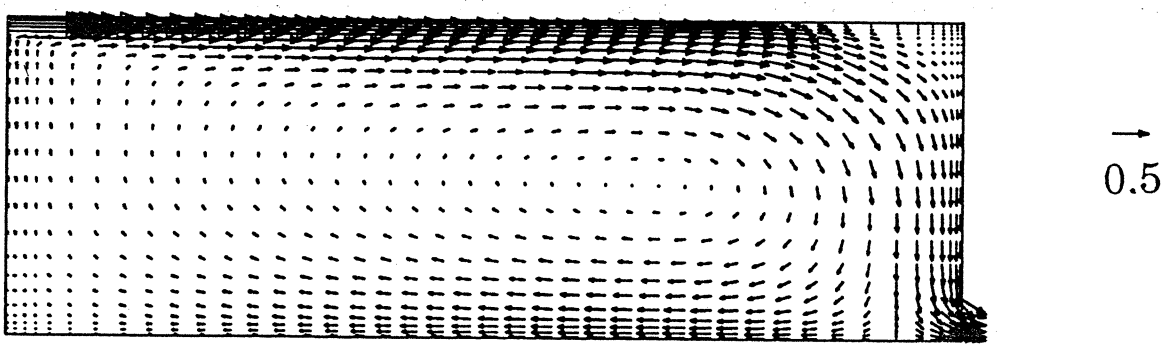

Figure 2. Velocity vectors of the isothermal case.

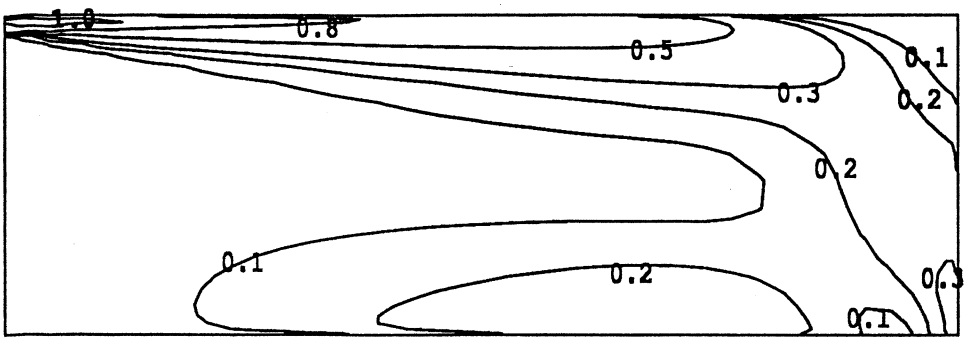

Figure 3. Air speed contours of the isothermal case.

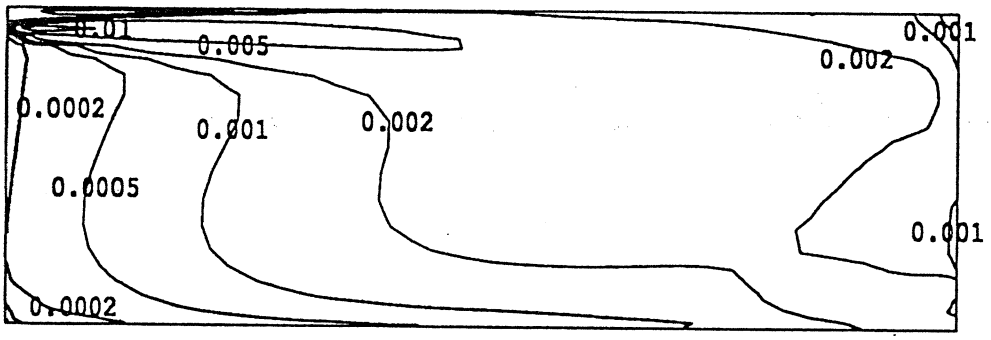

Figure 4. Contours of turbulent kinetic energy (m^2/s^2) in the isothermal case.

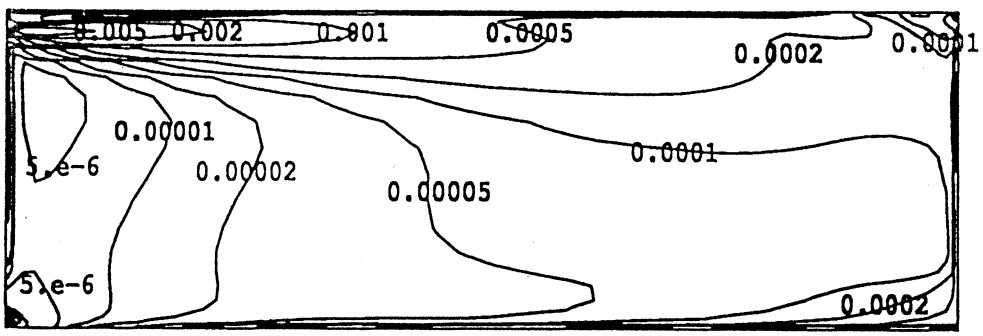

Figure 5. Contours of dissipation ε (m^2/s^3) in the isothermal case.

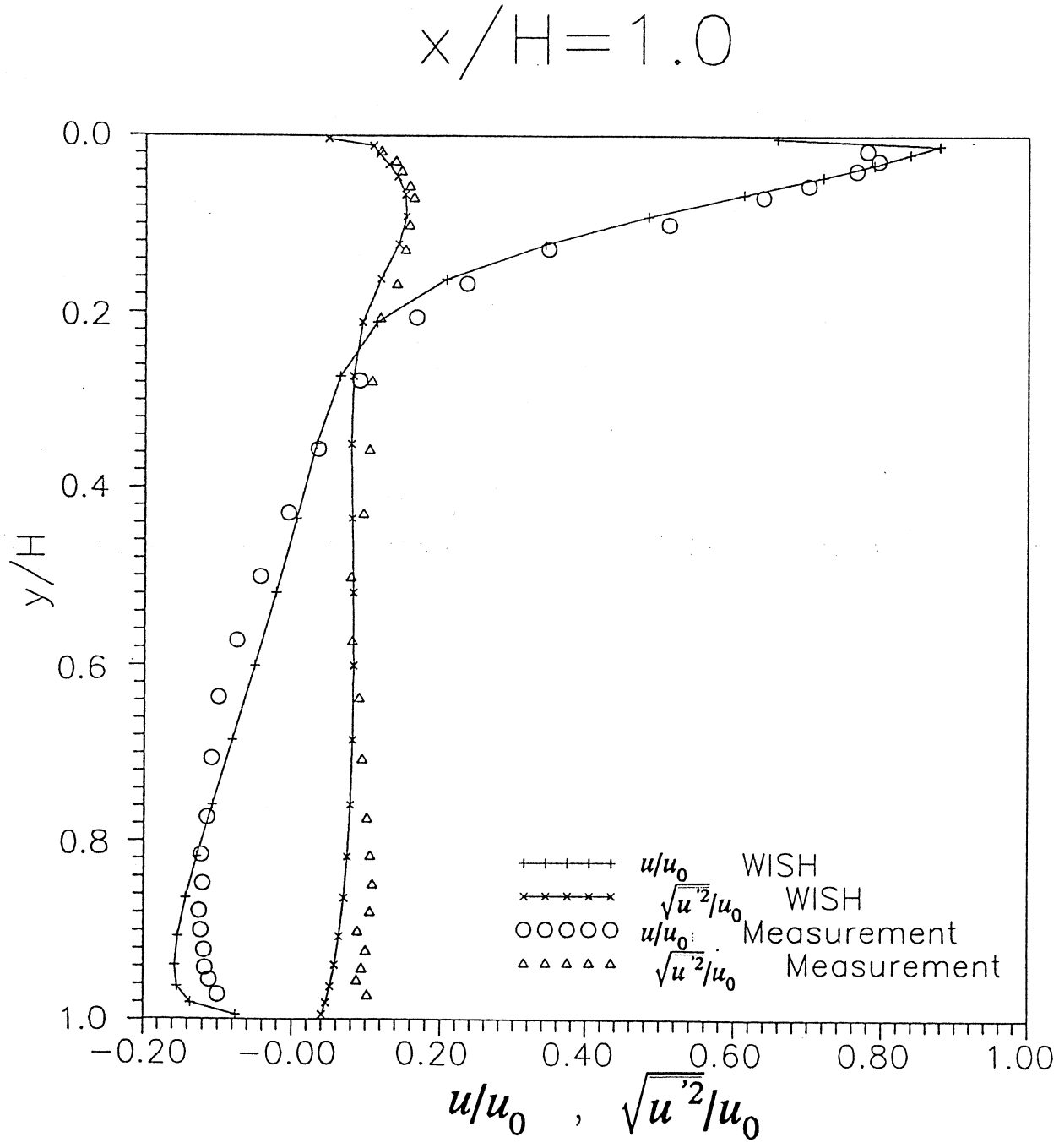

Figure 6. Comparison of the computed and measured mean velocity and turbulent intensity in the isothermal case in section x/H = 1.0.

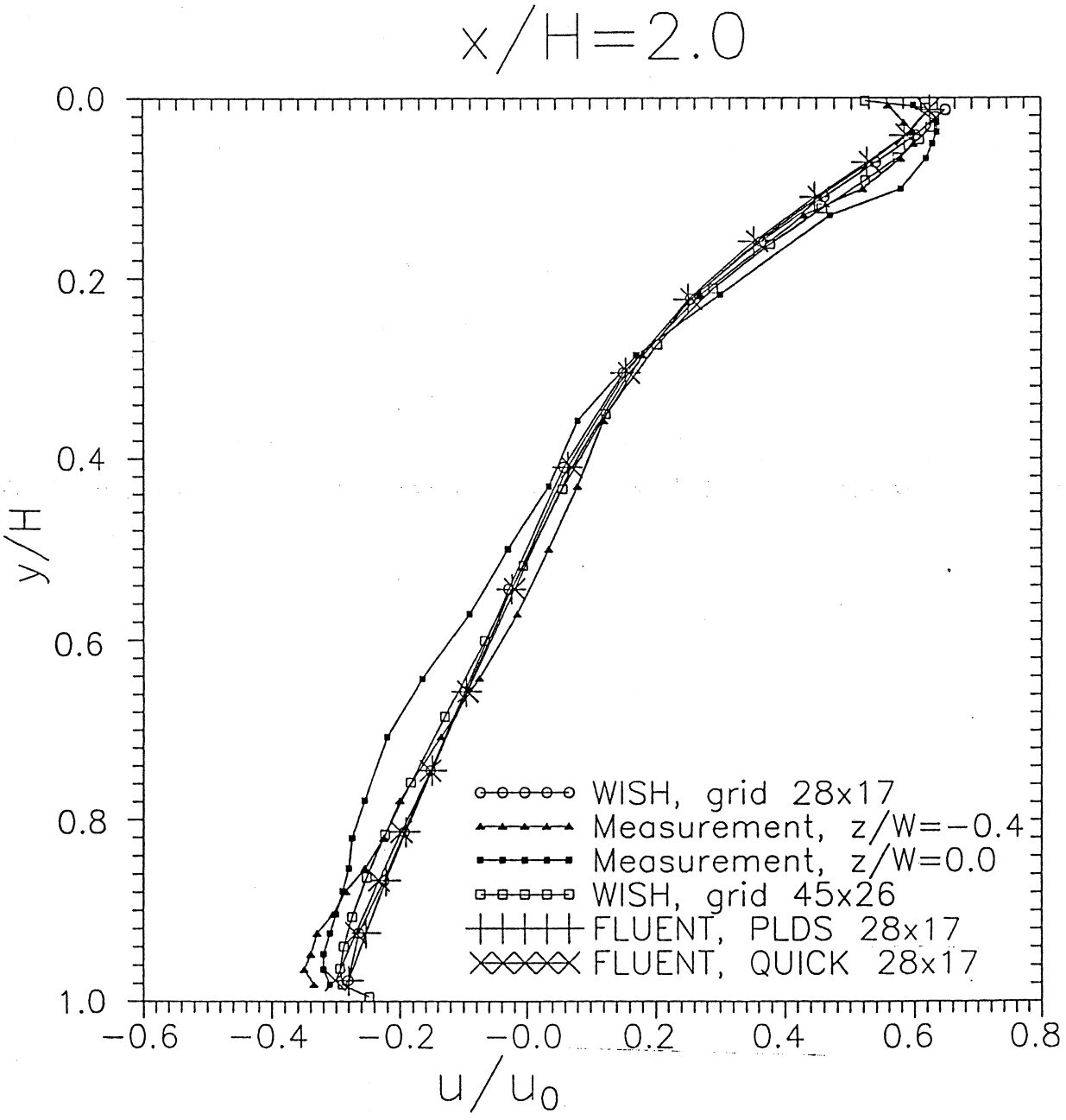

Figure 7. Comparison of the computed and measured mean velocity in the isothermal case in section x/H = 2.0.

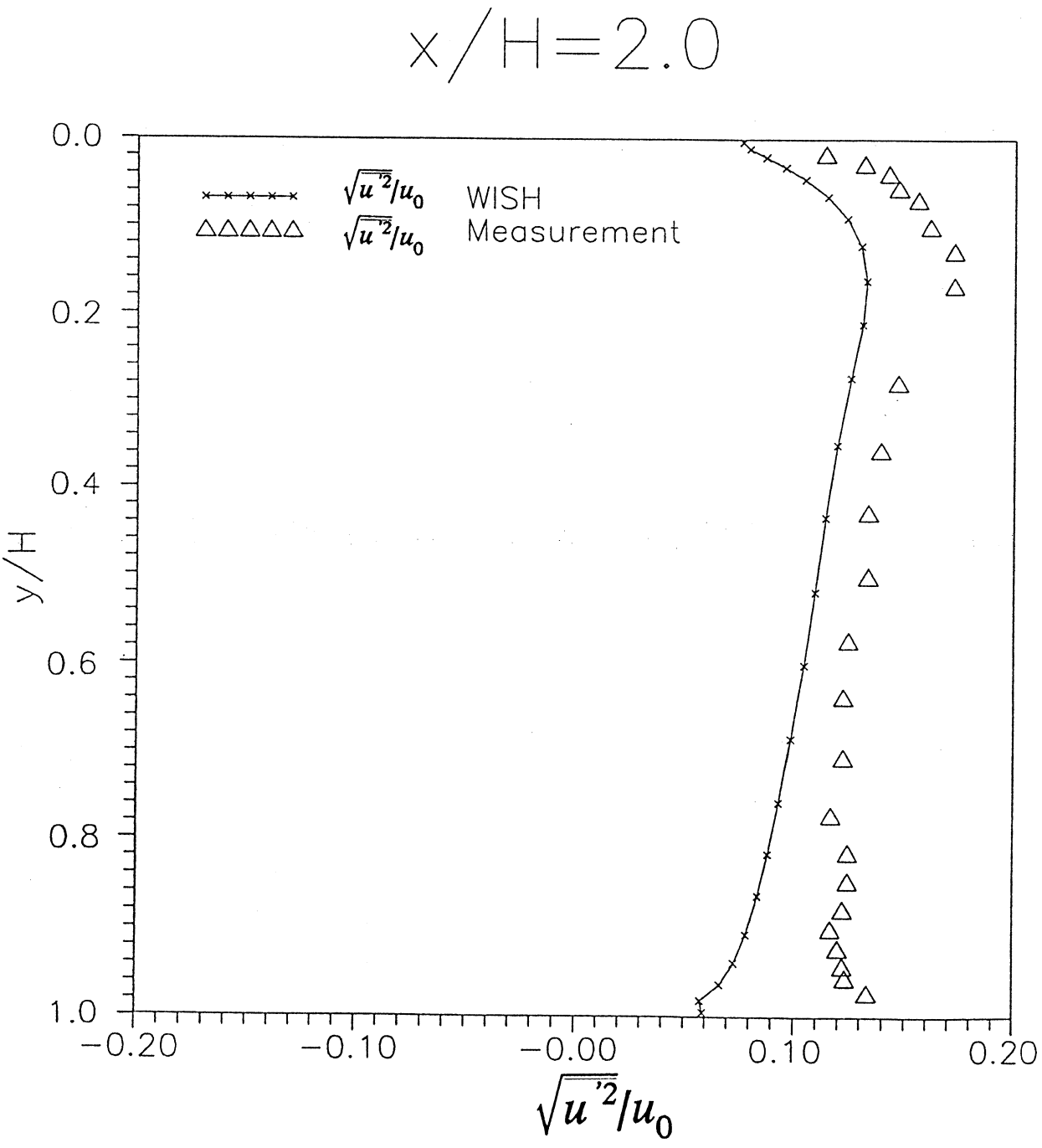

Figure 8. Comparison of the computed and measured turbulent intensity in the isothermal case in section x/H = 2.0.

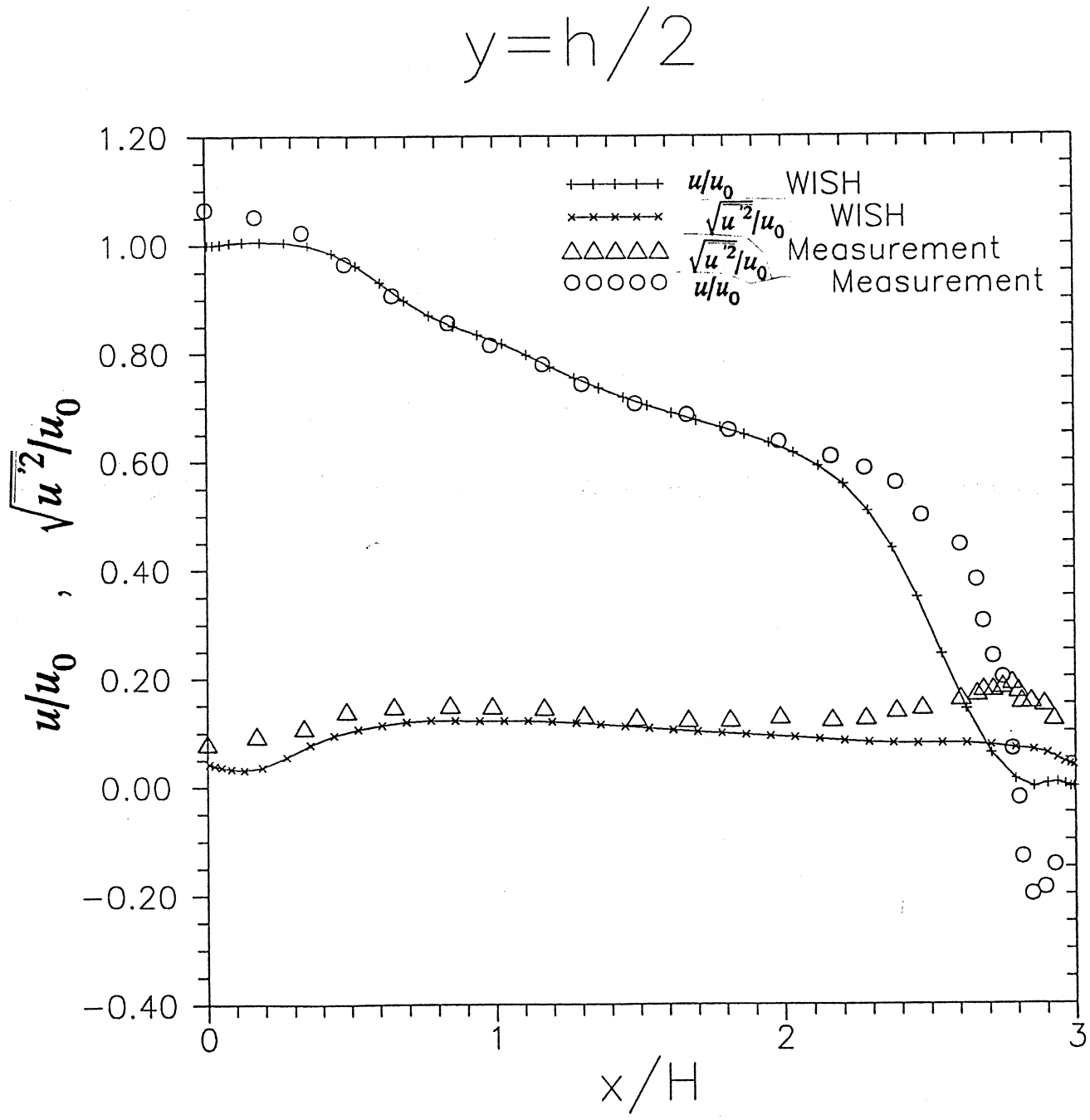

Figure 9. Comparison of the computed and measured mean velocity and turbulent intensity in the isothermal case in section y = h/2.

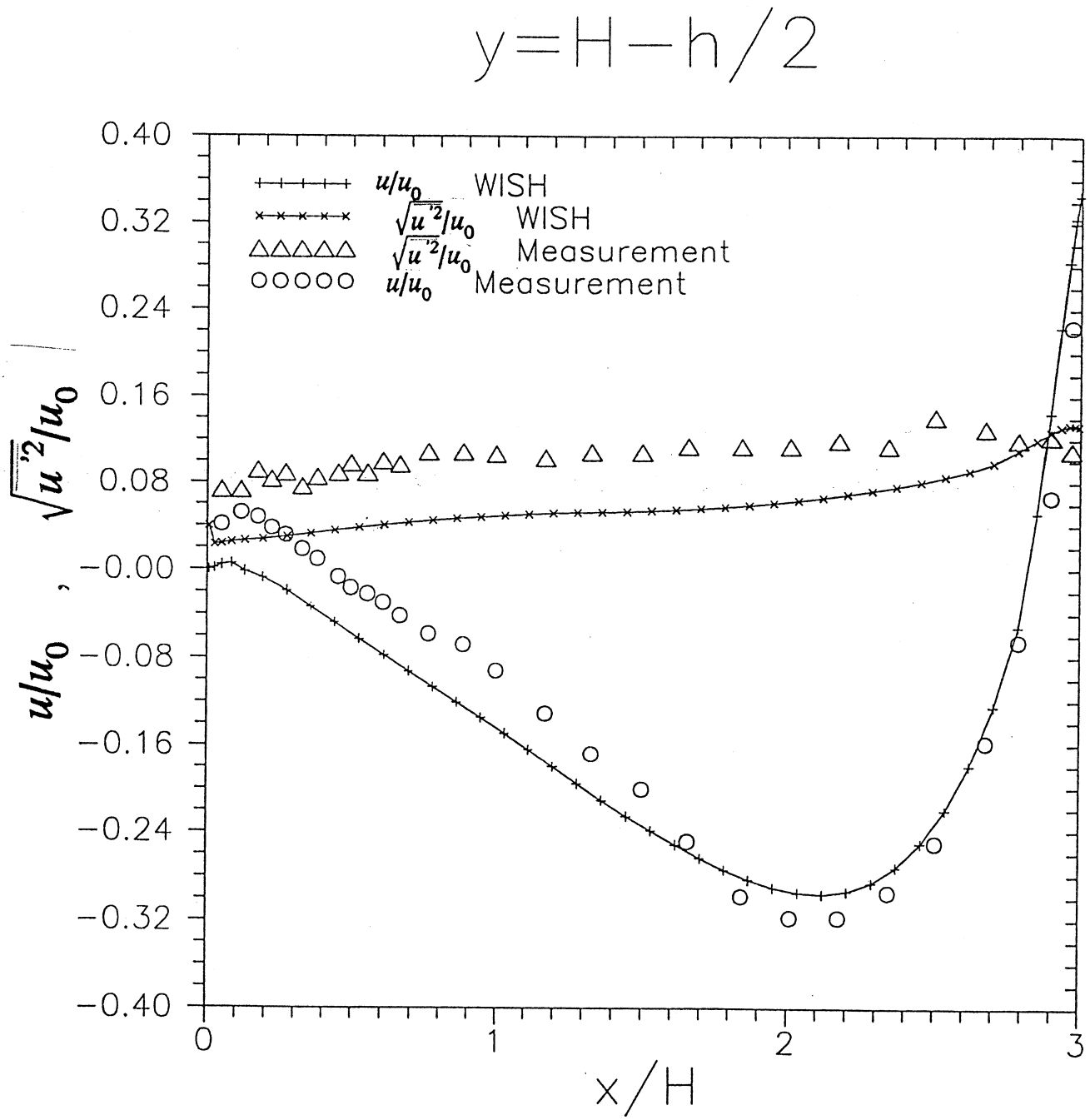

Figure 10. Comparison of the computed and measured mean velocity and turbulent intensity in the isothermal case in section y = H - h/2.

4.1 Grid and differencing scheme influence

Velocity profiles at x/H = 2 have been plotted in Figure 7. Computed results with a coarser grid (28x17 = 476 points) and the same differencing schemes as in an earlier report (Heikkinen & Piira 1990) are also shown. The fine grid profile seems to be closer to the measured profile. Different coarse grid profiles are close to each other, except near the walls where differences can be seen, maybe better from Tables 2 and 3.

Table 2. Maximum velocity u/u0 in the jet near the ceiling at x/H = 2 using different grids and differencing schemes.

	Grid 28x17	*Grid 45x26*	*Difference*
WISH, upwind scheme	*0.651*	*0.634*	*-2.6 %*
FLUENT, power law scheme	*0.626*	*0.610*	*-2.6 %*
FLUENT, QUICK scheme	*0.624*	*0.612*	*-1.9 %*

Table 3. Maximum velocity u/u0 near the floor at x/H = 2 using different grids and differencing schemes.

	Grid 28x17	*Grid 45x26*	*Difference*
WISH, upwind scheme	*-0.281*	*-0.294*	*4.6 %*
FLUENT, power law scheme	*-0.280*	*-0.290*	*3.6 %*
FLUENT, QUICK scheme	*-0.301*	*-0.288*	*-4.3 %*

Near the ceiling, Wish predicts 4 % higher velocities than Fluent with the power law scheme but near the floor the differences are less than 2 %. The difference between power law and QUICK near the ceiling is small, as expected, because numerical diffusion is not a problem in the jet region. But near the floor, the QUICK scheme predicts a 7 % higher velocity than the power law scheme when the coarse grid is used. With the fine grid, differences with all predictions near the floor are small.

The fact that the biggest velocities near the floor were obtained with a coarse grid and the QUICK scheme was also true in 3-dimensional simulations (Heikkinen & Piira, 1990). In both 2- and 3-dimensional computations the coarse grid was constructed so that logarithmic wall function rules (y+ between 30 and 100) were not violated, see Table 4. With the fine grid the y+ values are low and therefore the shear stress is too high, which means loss of momentum and low velocities.

Table 4. Mean y+ values at the first grid point near the surface with the coarse grid and the fine grid. From Wish computations.

	Grid 28x17	*Grid 45x26*
Ceiling	*63*	*11*
Floor	*93*	*15*
East wall	*61*	*17*
West wall	*40*	*10*

4. RESULTS OF THE NON-ISOTHERMAL TEST CASE

Predictions were repeated with different Archimedes numbers from 0.04 to 0.24 with 0.04 intervals to find the penetration depth at each Archimedes number, as suggested by Nielsen (1990). It turned out that penetration depth is practically the same as the room length with Archimedes numbers 0.12 or less. With Archimedes numbers 0.16 and higher, the penetration depth is nearly zero (see Fig. 11). Penetration depths between 0 and L were not found as in experiments (Nielsen 1990).

Other penetration depths do appear during the iteration. An example is given in Fig. 12, where the penetration depth moves from left to right during the computation. If one looks at the residuals of different equations (Fig. 13), one would be tempted to stop calculation after 3000 iterations, when the penetration depth is about 0.25 and the flow field is still changing. This means that we have to be careful with convergence criteria in cases which are not very stable. It is a good practise to look at changes of air flow patterns during the iteration. Also changes at a good monitoring point will reveal changes in the flow field.

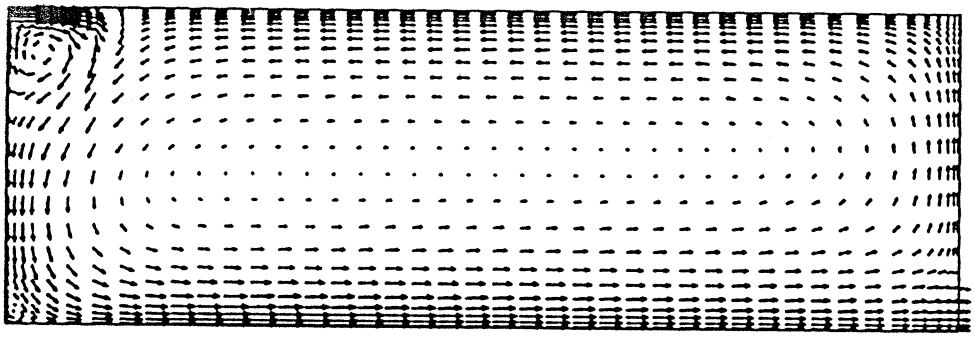

1

Figure 11. Velocity vectors of the non-isothermal case when Ar = 0.16.

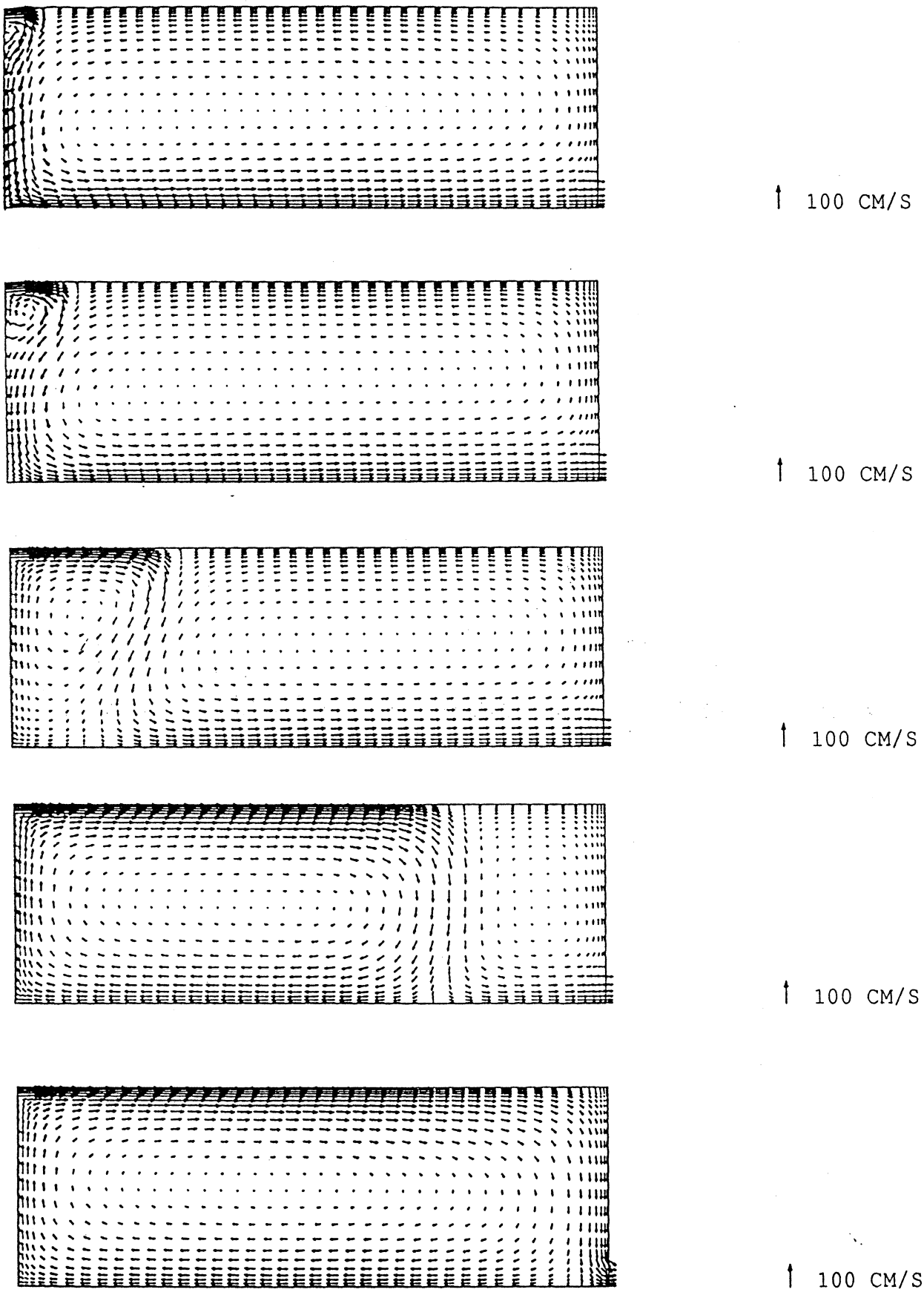

Figure 12. Air flow patterns at iteration numbers 500 (upper figure), 2000, 3000, 4000 and 6000 (lower figure), Ar = 0.08. The residuals are shown in Figure 13.

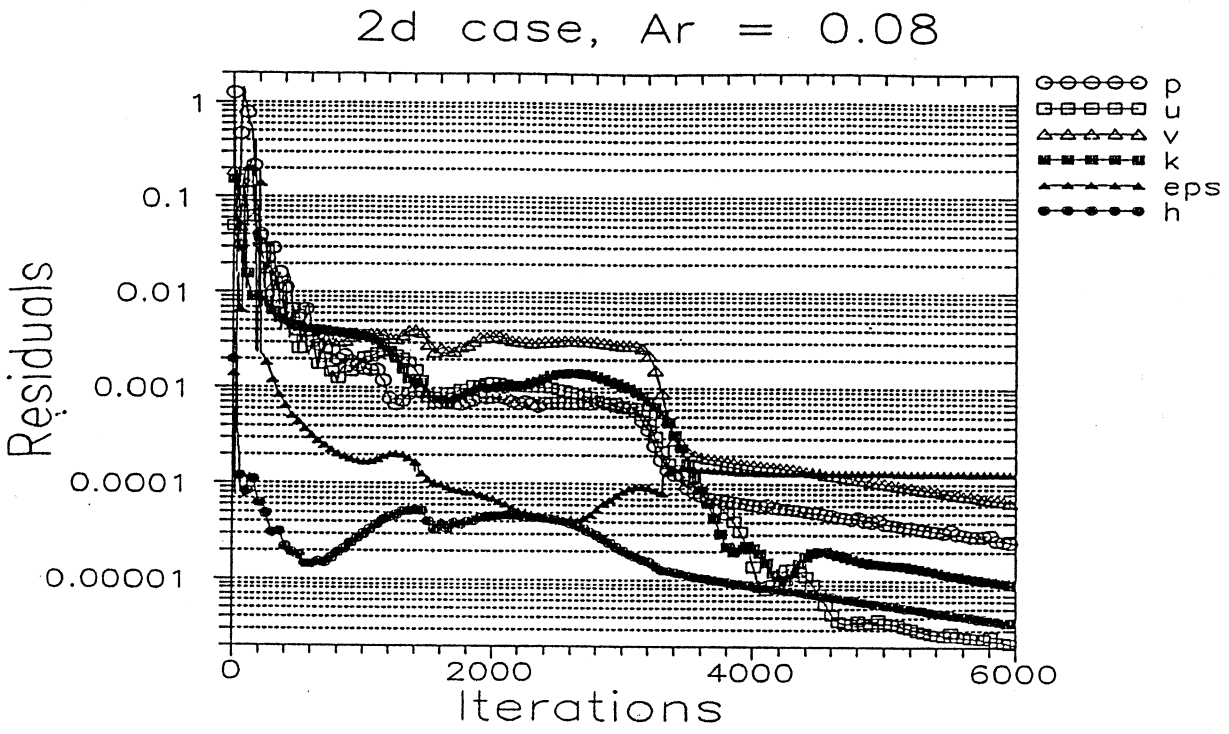

Figure 13. The residuals of u, v, p, k, ε and h in the non-isothermal case when Ar = 0,08.

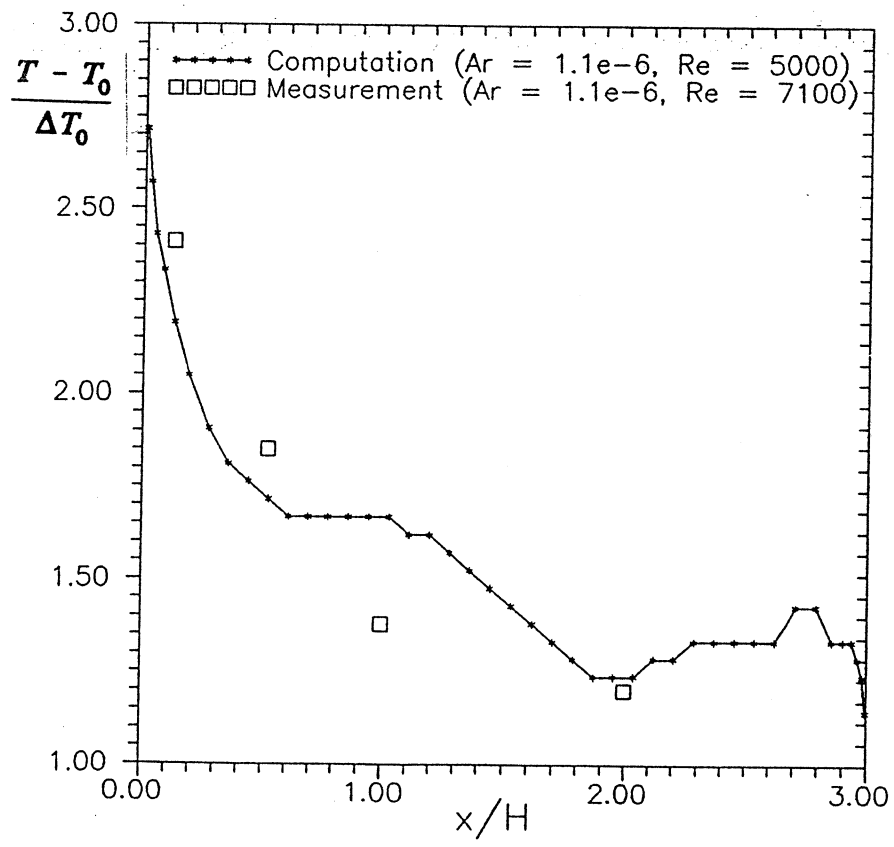

Figure 14. Comparison of the computed and measured temperature in the non-isothermal case in section y/H = 0.75 with a very low Archimedes number.

CONCLUSIONS

In the isothermal case the air flow patterns in the computations and in the measurements were very similar. However, recirculation areas near the corners were not well predicted.

Computations with a fine grid very close to the walls and therefore violating the rules of logarithmic wall functions gave the best general agreement with the measurements. However, a computation with a coarser grid and numerically more accurate method (QUICK differencing scheme) gave the best maximum velocity prediction near the floor. This velocity was still 6 % lower than the measured velocity. The grid and differencing scheme effects were similar to those in earlier three-dimensional computations.

In the non-isothermal case the penetration depth could not be predicted. One should be careful in simulating air flow patterns which are not clearly stable.

REFERENCES

Creare Inc. 1987. Fluent, a general purpose computer program for modeling fluid flow, heat transfer and combustion. Hanover NH, seminar notes.

Heikkinen, J, Piira, K. 1990. Simulation of test case B (forced convection, isothermal). IEA Annex 20, research item 1.19SF, working report

Launder, B.E, Spalding, D.B. 1974. The numerical computation of turbulent flows. Computer methods in mechanics and engineering, 3, p. 269 -289.

Lemaire, A.D. 1989b. User manual WISH. TNO - Institute of Applied Physics, Delft.

Nielsen. P.V. 1990. Specification of a two-dimensional test case. Aalborg University. ISSN 0902-7513 R9040, Aalborg.

Patankar, S.V, 1980. Numerical Heat Transfer and Fluid Flow. McGraw-Hill, New York.